

Supporting Information

Enhanced Oxygen Evolution Reaction Activity on Two-Dimensional vdW Ferromagnetic Cr₂Ge₂Te₆ Through A Two-Active-Sites Synergism

Zongxiang Kang, Wei Su, Qihong Li, Jingguo Hu, Jing Pan*

College of Physics Science and Technology, Yangzhou University, Yangzhou, 225002, China

The comparison of GGA and GGA+U methods

Table S1. The calculated lattice parameters and band gap of Cr₂Ge₂Te₆ calculated by GGA and GGA+U methods.

| Cr ₂ Ge ₂ Te ₆ | Experimental value | GGA | GGA+U (1 eV) | GGA+U (3 eV) |
|---|--------------------|-------|--------------|--------------|
| $a = b$ (Å) | 6.82 | 6.80 | 6.81 | 6.96 |
| c (Å) | 20.56 | 20.44 | 20.44 | 22.54 |
| E_g (bulk) (eV) | 0.38 | 0.23 | 0.29 | 0.20 |

To verify the reliability of GGA + U method with $U = 1.0$ eV, we compare our calculated lattice constants and band gap of the bulk Cr₂Ge₂Te₆ with GGA, GGA + U ($U = 3$ eV) calculated results and the experimental results in Table S1. The comparative results show that the GGA + U ($U = 1$ eV) calculated structural parameters are $a = b = 6.81$ Å, $c = 20.44$ Å, in very good agreement with the experimental values ($a = b = 6.82$ Å, $c = 20.56$ Å). As shown in Figure S1(a), the bulk Cr₂Ge₂Te₆ has a layered structure. Additionally, the band structure calculation as shown in Figure S1(b) shows that the bulk Cr₂Ge₂Te₆ is indirect band gap semiconductor with the band gap of 0.29 eV, which is also in good agreement with the experimental band gap of 0.38 eV.

* Corresponding author. Email: jp@yzu.edu.cn

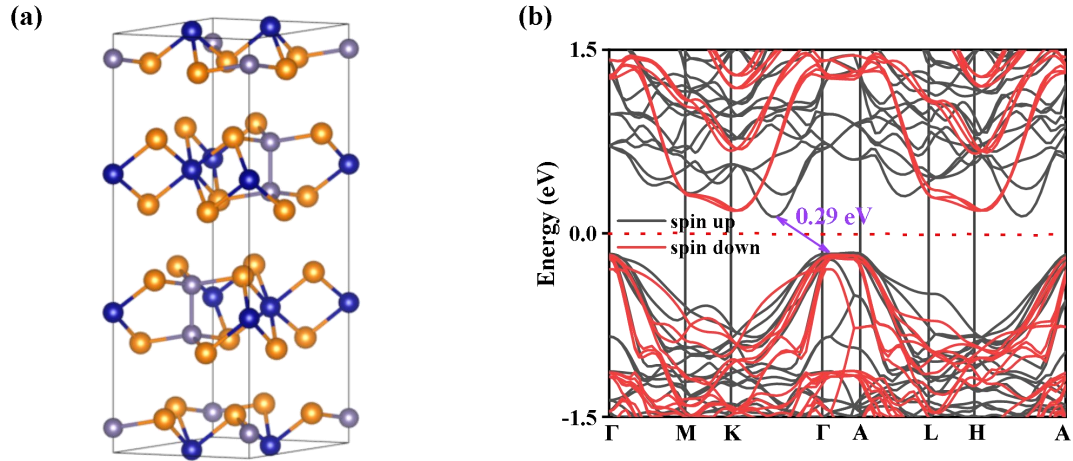


Figure S1. (a) Crystal structure of the bulk $\text{Cr}_2\text{Ge}_2\text{Te}_6$. (b) The calculated band structure of the bulk $\text{Cr}_2\text{Ge}_2\text{Te}_6$.

The magnetic ground states of the monolayer $\text{Cr}_2\text{Ge}_2\text{Te}_6$

In order to investigate the magnetic ground state of the monolayer $\text{Cr}_2\text{Ge}_2\text{Te}_6$, we take into account four magnetic states as shown in Figure S1[1]: ferromagnetic (FM) state, Néel antiferromagnetic (AFM) state, Stripy antiferromagnetic state, and Zigzag ferromagnetic state, respectively. An FM state means all the spins on the lattice point is along the same direction. While an AFM states require opposite aligning of neighboring spins on different sublattices[2]. The calculations show that the magnetic ground state of the $\text{Cr}_2\text{Ge}_2\text{Te}_6$ is FM state because the total energy of FM configuration is the lowest.

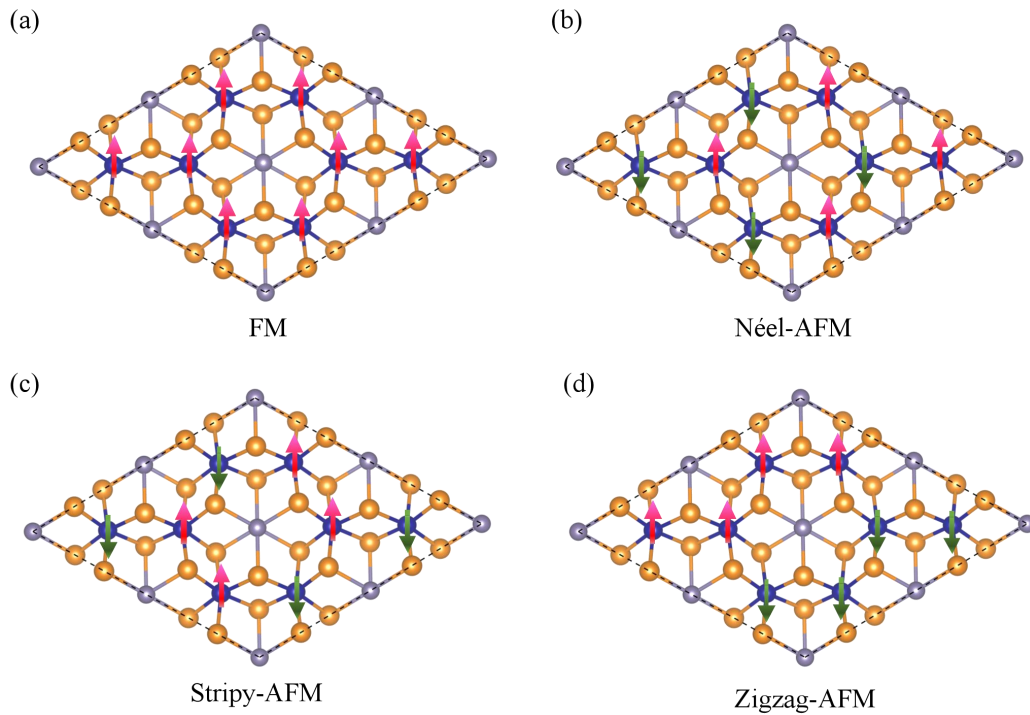


Figure S2. Schematics of four different magnetic structures: (a) FM, (b) Néel-AFM, (c) Stripy-AFM, and (d) Zigzag-AFM. The red and green arrows represent up and down spins, respectively.

The band structure of the $\text{Cr}_2\text{Ge}_2\text{Te}_6$ for HO^* , O^* , HOO^* and O_2 adsorption along the pathway I

In order to study the effect of the oxygen-containing intermediates adsorption on the $\text{Cr}_2\text{Ge}_2\text{Te}_6$, we calculated the band structures of HO^* , O^* , HOO^* and O_2 adsorbed $\text{Cr}_2\text{Ge}_2\text{Te}_6$. Our results show that the intermediates adsorbed $\text{Cr}_2\text{Ge}_2\text{Te}_6$ remain exhibit magnetism due to the asymmetry between the spin-up and spin-down channels. For HO^* adsorption, the band gap of $\text{Cr}_2\text{Ge}_2\text{Te}_6$ gradually decreases, and for O^* , HOO^* and O_2 adsorption, the band gaps of the $\text{Cr}_2\text{Ge}_2\text{Te}_6$ decrease to 0.37, 0.32 and 0.4 eV, which is much lower than that of pure $\text{Cr}_2\text{Ge}_2\text{Te}_6$ (0.53 eV).

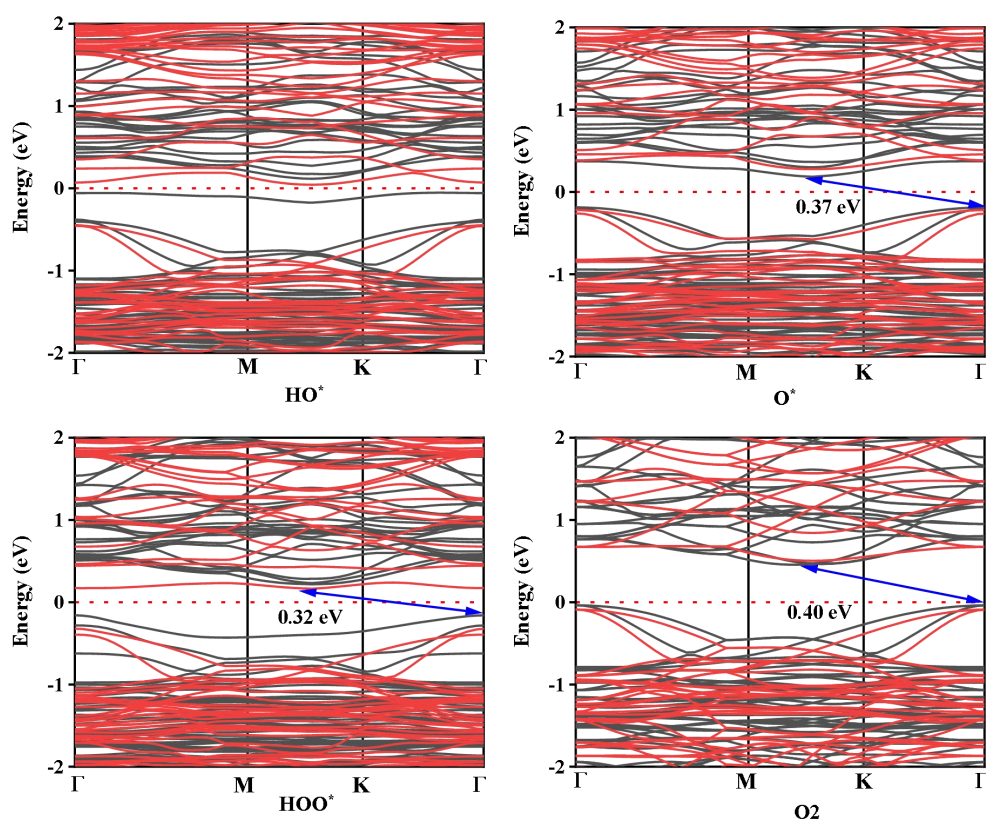


Figure S3. The calculated band structures of four oxygen-containing intermediates: (a) HO^* , (b) O^* , (c) HOO^* and (d) O_2 adsorbed $\text{Cr}_2\text{Ge}_2\text{Te}_6$ along pathway I.

The band structure of the $\text{Cr}_2\text{Ge}_2\text{Te}_6$ for HO^* , 2HO^* , $\text{O}^* + \text{HO}^*$ and O_2 adsorption along the pathway II

The results show that for HO^* , 2HO^* and $\text{O}^* + \text{HO}^*$ adsorption, the band gap of $\text{Cr}_2\text{Ge}_2\text{Te}_6$ gradually decreases. For O_2 adsorption, the band gap of $\text{Cr}_2\text{Ge}_2\text{Te}_6$ is 0.4 eV.

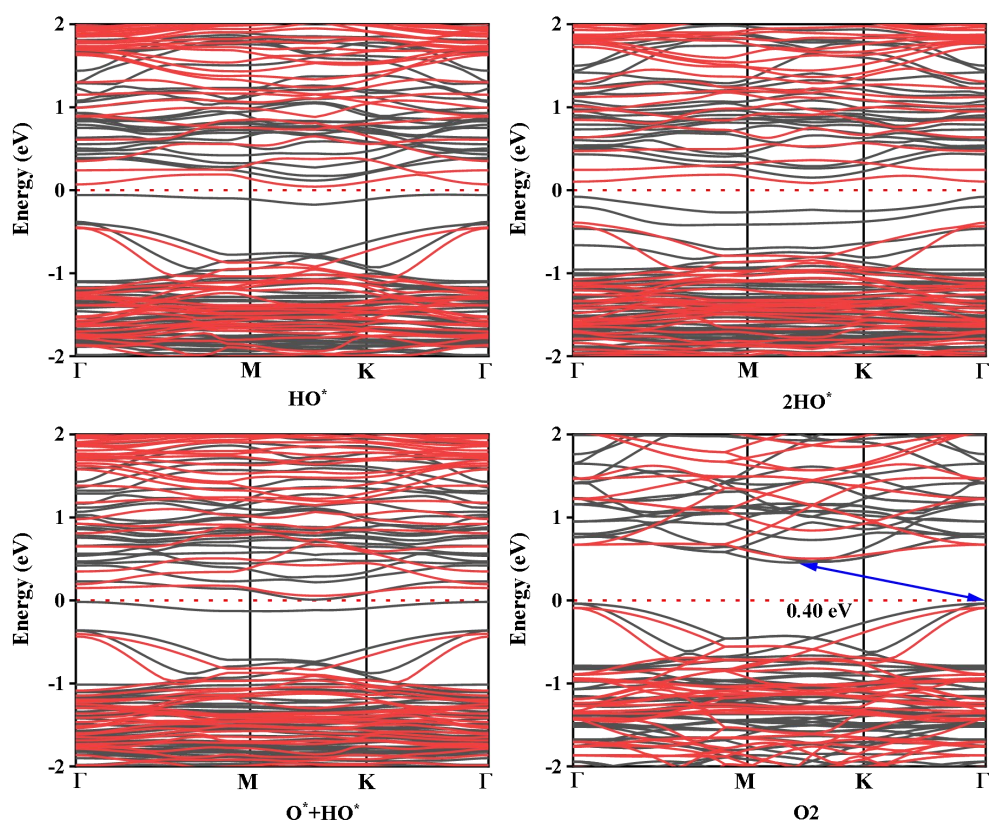


Figure S4. The calculated band structures of four oxygen-containing intermediates: (a) HO^* , (b) 2HO^* , (c) $\text{O}^* + \text{HO}^*$ and (d) O_2 adsorbed $\text{Cr}_2\text{Ge}_2\text{Te}_6$ along pathway II.

The band structure of the $\text{Cr}_2\text{Ge}_2\text{Te}_6$ for HO^* , 2HO^* , $\text{O}^* + \text{HO}^*$ and O_2 adsorption along the pathway III

The results show that $\text{Cr}_2\text{Ge}_2\text{Te}_6$ gradually exhibits metallicity for HO^* and $\text{O}^* + \text{HO}^*$ adsorption. For O^* and O_2 adsorption, the band gaps of $\text{Cr}_2\text{Ge}_2\text{Te}_6$ are 0.37 and 0.40 eV.

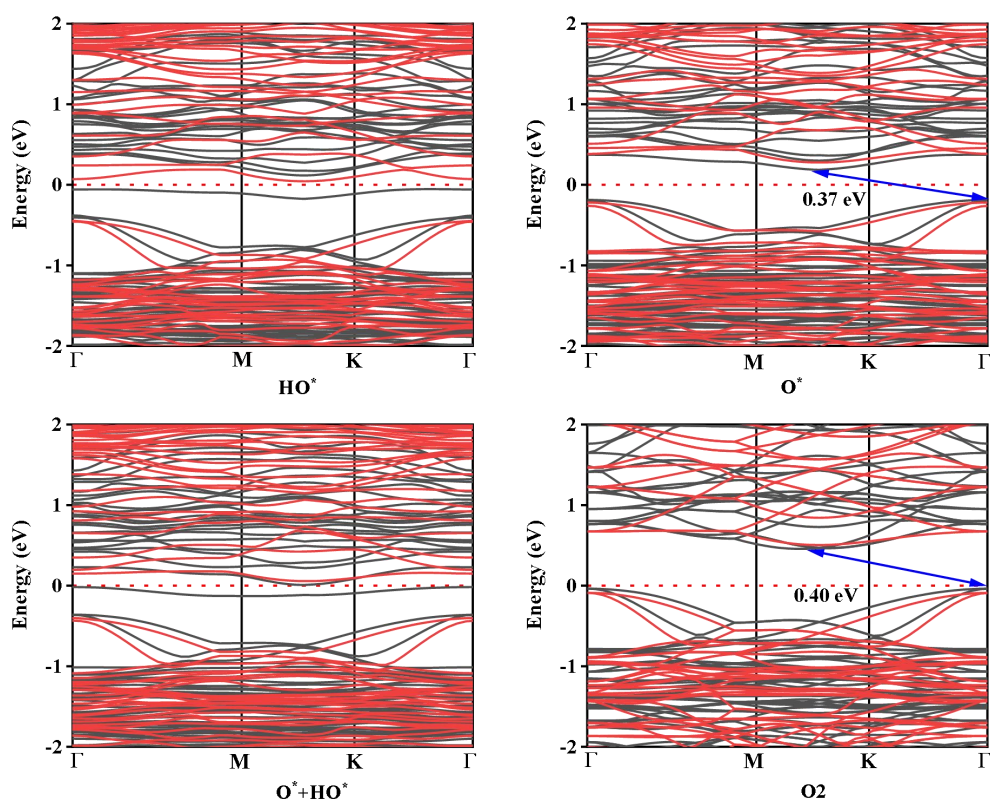


Figure S5. The calculated band structures of four oxygen-containing intermediates: (a) HO^* , (b) O^* , (c) $\text{O}^* + \text{HO}^*$ and (d) O_2 adsorbed $\text{Cr}_2\text{Ge}_2\text{Te}_6$ along pathway III.

REFERENCES

1. Kang, W., et al., Two-dimensional half-metallicity in transition metal atoms decorated $\text{Cr}_2\text{Ge}_2\text{Te}_6$. *Frontiers in Physics*, 2023. 11.
2. Zhang, S., et al., Two-dimensional magnetic materials: structures, properties and external controls. *Nanoscale*, 2021. 13(3): p. 1398-1424.